Activation of the Propargylic C−H Bond and Formation of the Unsaturated C_3S_2 Five-Membered Rings on the RuSSRu Core

Hiroyasu Sugiyama, Yoshihiro Moriya, and Kazuko Matsumoto*

Department of Chemistry, School of Science and Engineering, and Advanced Research Institute of Science and Technology, Waseda University, and Japan Science and Technology Corporation, 3-4-1 Ohkubo, Shinjuku, Tokyo 169-8555, Japan

Received July 20, 2001

The reactions of the disulfide-bridged dinuclear Ru^{III} complex $[\{Ru(P(OCH_3)_3)_2(CH_3CN)_3\}_2(\mu\text{-}S_2)](CF_3SO_3)_4$ (**1**) with terminal and internal alkynes gave $[\{Ru(P(OCH_3)_3)_2(CH_3CN)_3\}_2(\mu\text{-}SCR^1{=}CHCHR^2S)](CF_3SO_3)_4$ (**2**, $R^1 = H$, $R^2 = SC_6H_5$; **3**, $R^1 = H$, $R^2 = C_2H_5$; **4**, $R^1 = CH_3$, $R^2 = H$; **5**, $R^1 = C_2H_5$, $R^2 = CH_3$, **6**, $R^1 = C_6H_5$, $R^2 = H$), in which an unsaturated C_3S_2 five-membered ring is formed via activation of the propargylic C−H bond. Treatment of **1** with an unsymmetric alkyne, 2-pentyne, gave a mixture of $[\{Ru(P(OCH_3)_3)_2(CH_3CN)_3\}_2(\mu\text{-}SC(CH_3){=}CHCH(CH_3)S)](CF_3SO_3)_4$ (**7**) and $[\{Ru(P(OCH_3)_3)_2(CH_3CN)_3\}_2(\mu\text{-}SC(CH_2CH_3){=}CHCH_2S)](CF_3SO_3)_4$ (**8**), which corresponds to the activation of secondary and primary propargylic C−H bonds, respectively. The reaction at 0 °C preferably gave **7**, whereas **8** was obtained as the major component at 40 °C.

Introduction

Synthesis of the active centers of the biomolecules has been one of the most important research targets of transition metal sulfur chemistry. Among such active centers, molybdopterin, having a dithiolene ligand coordinated to the molybdenum center, has been widely investigated.[1] In the biomimetic approach to the molybdopterin, reaction of transition metal sulfides with alkynes is widely used to synthesize the model metal−pterin complexes,[2] as well as the direct transmetalation of a dithiolene ligand to the metal center.[3] Actually, many types of inorganic sulfur ligands on the transition metal center undergo [2+3] cycloaddition reactions with alkynes to give the dithiolene complexes.[4−11] It is also reported that $[\{(S_2)MoS\}_2(\mu\text{-}S)_2]^{2-}$ reacts with RC≡CR (R = $COOCH_3$) to give $[\{(SSCR{=}CR)MoS\}_2(\mu\text{-}S)_2]^{2-}$, where the alkyne is inserted into the Mo−S bond.[12] The alkynes used in these reactions are usually activated by the electron-withdrawing groups such as COOR, CF_3, and C_6H_5. Nonactivated alkynes usually do not react, and the starting complex is regarded as very reactive, if it reacts with phenyl-substituted alkynes such as $C_6H_5C{\equiv}CC_6H_5$ and $C_6H_5C{\equiv}CH$. On the other hand, alkenyl carbon atoms are considerably less reactive toward these metal sulfide complexes. Actually, the very limited sulfide complexes are reactive enough to react with alkenes, for instance ReS_4^- [13] and $(CpMo)_2(\mu\text{-}S_2CH_2)(\mu\text{-}S_2)$.[14] As a summary, almost all of the previously known C−S bond formation reactions were found only with relatively reactive substrates.

We reported previously that the reaction of $[\{Ru(P(OCH_3)_3)_2(CH_3CN)_3\}_2(\mu\text{-}S_2)](CF_3SO_3)_4$ (**1**) with alkenes gives various C_3S_2-ring bridging ligands, and in all of these reactions, activation of the allylic C−H bond is the common intial key step.[15] The reaction mechanism suggests that the bridging disulfide ligand having double bond nature cleaves the allylic C−H

* Corresponding author. E-mail: kmatsu@mn.waseda.ac.jp. Tel: +81-3-5286-3108. Fax: +81-3-5273-3489.

(1) (a) Kilpatrick, L.; Rajagopalan, K. V.; Hilton, J.; Bastian, N. R.; Stiefel, E. I.; Pilato, R. S.; Spiro, T. G. *Biochemistry* **1995**, *34*, 3032. (b) Stiefel, E. I. *J. Chem. Soc., Dalton Trans.* **1997**, 3915.

(2) Pilato, R. S.; Eriksen, K. A.; Greaney, M. A.; Stiefel, E. I.; Goswami, S.; Kilpatrick, L.; Spiro, T. G.; Taylor, E. C.; Rheingold, A. L. *J. Am. Chem. Soc.* **1991**, *113*, 9372.

(3) Fisher, B.; Enemark, J. H.; Basu, P. *J. Inorg. Biochem.* **1998**, *72*, 13.

(4) (a) Goodman, J. T.; Inomata, S.; Rauchfuss, T. B. *J. Am. Chem. Soc.* **1996**, *118*, 11674. (b) Goodman, J. T.; Rauchfuss, T. B. *Inorg. Chem.* **1998**, *37*, 5740.

(5) (a) Kawaguchi, H.; Tatsumi, K. *J. Am. Chem. Soc.* **1995**, *117*, 3885. (b) Kawaguchi, H.; Yamada, K.; Lang, J.-P.; Tatsumi, K. *J. Am. Chem. Soc.* **1997**, *119*, 10346.

(6) Shibahara, T.; Sakene, G.; Mochida, S. *J. Am. Chem. Soc.* **1993**, *115*, 10408.

(7) Rakowski DuBois, M.; Jagirdar, B. R.; Dietz, S.; Noll, B. C. *Organometallics* **1997**, *16*, 294.

(8) Bolinger, C. M.; Rauchfuss, T. B. *Inorg. Chem.* **1982**, *21*, 3947.

(9) Draganjac, M.; Coucouvanis, D. *J. Am. Chem. Soc.* **1983**, *105*, 139.

(10) Weberg, R.; Haltiwanger, R. C.; Rakowski Dubois, M. *Organometallics* **1985**, *4*, 1315.

(11) Inomata, S.; Hiyama, K.; Tobita, H.; Ogino, H. *Inorg. Chem.* **1994**, *33*, 5337.

(12) Halbert, T. R.; Pan, W.-E.; Stiefel, E. I. *J. Am. Chem. Soc.* **1983**, *105*, 5476.

(13) Goodman, J. T.; Rauchfuss, T. B. *J. Am. Chem. Soc.* **1999**, *121*, 5017.

(14) (a) McKenna, M.; Wright, L. L.; Miller, D. J.; Tanner, L.; Haltiwanger, R. C.; Rakowski DuBois, M. *J. Am. Chem. Soc.* **1983**, *105*, 5329. (b) Birnbaum, J.; Laurie, J. C. V.; Rakowski DuBois, M. *Organometallics* **1990**, *9*, 156. (c) Birnbaum, J.; Haltiwanger, R. C.; Bernatis, P.; Teachout, C.; Parker, K.; Rakowski DuBois, M. *Organometallics* **1991**, *10*, 1779. (d) Koval, C. R.; Lopez, L. L.; Kaul, B. B.; Renshaw, S. Green, K.; Rakowski DuBois, M. *Organometallics* **1995**, *14*, 3440.

(15) (a) Hossain, Md. M.; Lin, Y.-S.; Sugiyama, H.; Matsumoto, K. *J. Am. Chem. Soc.* **2000**, *122*, 172. (b) Sugiyama, H.; Hossain, Md. M.; Lin, Y.-S.; Matsumoto, K. *Inorg. Chem.*, in press.

10.1021/om0106534 CCC: $20.00
Publication on Web 11/29/2001

bond like the transition metal centers in organometallic complexes. The Ru centers may assist the reaction by adjusting the electronic state of the S_2 ligand and fixing the alkene molecule by coordination. Since the C−H bond activation is the initial and rate-determining step, the reaction depends on the reactivity of the allylic C−H bond rather than that of the C=C double bond. The different nature of the C=C double bonds gives several different subsequent steps resulting in a variety of products. It is noteworthy that C−H activation proceeds very smoothly on the disulfide bridging ligand at room temperature. Since the propargylic C−H bond has some similar reactivity to allylic C−H bonds, the reactivity of the propargylic C−H bond toward **1** and the related compound is studied in the present work.

Experimental Section

All the experiments were carried out under nitrogen or argon, by using standard Schlenk tube techniques or a glovebox. The solvent CD_3CN was dried over CaH_2 and purified by trap-to-trap distillation prior to use. Other solvents that were purchased dry were used without further purification. The NMR spectra were recorded on a JEOL Lambda 270 spectrometer, operating at 270 MHz for ^1H and 109 MHz for ^{31}P. The chemical shifts are reported in δ unit (ppm) downfield from Me_4Si for ^1H and from H_3PO_4 (85%, external reference) for ^{31}P. All the carbon, hydrogen, and nitrogen analyses were carried out on a Perkin-Elmer PE 2400II elemental analyzer.

Synthesis of [{Ru(P(OCH$_3$)$_3$)$_2$(CH$_3$CN)$_3$}$_2${μ-SCH=CHCH(R)S}](CF$_3$SO$_3$)$_4$ (2, R = C$_6$H$_5$, 3, R = C$_2$H$_5$). To a CH_3CN (1 mL) solution of [{Ru(P(OCH$_3$)$_3$)$_2$(CH$_3$CN)$_3$}$_2$(μ-S$_2$)](CF$_3$SO$_3$)$_4$ (**1**) (80.3 mg, 0.05 mmol) was added phenylpropargyl sulfide (0.3 mL). The color of the solution gradually turned from dark blue to brown. This reaction mixture was allowed to stir for 3 h at room temperature before the addition of Et_2O to form a brown gummy solid. The crude product was recrystallized from CH_3CN/DME to give yellow crystals of [{Ru(P(OCH$_3$)$_3$)$_2$(CH$_3$CN)$_3$}$_2${μ-SCH=CHCH(C$_6$H$_5$)S}](CF$_3$SO$_3$)$_4$ (**2**) in 63% yield. Anal. Calcd for $C_{37}H_{62}F_{12}N_6O_{24}P_4Ru_2S_7$: C, 25.34; H, 3.56; N, 4.79. Found: C, 25.16; H, 3.33; N, 4.61. ^1H NMR (270 MHz, CD_3CN): δ 1.95 (s, 12H, 4 CH_3CN), 2.47 (s, 3H, CH_3CN trans to S), 2.52 (s, 3H, CH_3CN trans to S), 6.12 (dd, $^3J_{H2H3}$ = 4 Hz, $^4J_{H1H3}$ = 1 Hz, 1H, H^3), 6.47 (dd, $^3J_{H1H2}$ = 6 Hz, $^4J_{H1H3}$ = 1 Hz, 1H, H^1), 6.92 (dd, 1H, H^2), 7.49−7.52 (m, 3H, C$_6H_5$), 7.60−7.64 (m, 2H, C$_6H_5$). $^{31}P\{^1H\}$ NMR (CD_3CN, 109 MHz): δ 123.9 and 124.3 (d, $^2J_{PP}$ = 79 Hz, 2*P*(OCH$_3$)$_3$), 124.5 and 126.2 (d, $^2J_{PP}$ = 80 Hz, 2*P*(OCH$_3$)$_3$). $^{13}C\{^1H\}$ NMR (68 MHz, CD_3CN): δ 4.6 (*C*H$_3$CN), 55.5−56.3 (P(O*C*H$_3$)$_3$), 79.7 (S*C*HSC$_6$H$_5$), 128.0 (S*C*H=CH), 133.4 (SCH=*C*H), 130.7, 131.0, 133.6, and 133.8 (*C*$_6$H$_5$).

Analogously, treatment of **1** (80.3 mg, 0.050 mmol) with 1-pentyne (0.5 mL) in CH_3CN (1 mL) gave [{Ru(P(OCH$_3$)$_3$)$_2$(CH$_3$CN)$_3$}$_2${μ-SCH=CHCH(C$_2$H$_5$)S}] (CF$_3$SO$_3$)$_4$ (**3**) (48.2 mg, 0.029 mmol, 58%), after workup. Anal. Calcd for $C_{33}H_{62}F_{12}N_6O_{24}P_4Ru_2S_2$: C, 23.69; H, 3.73; N, 5.02. Found: C, 23.71; H, 3.86; N, 4.69. ^1H NMR (270 MHz, CD_3CN): δ 1.10 (dt, J = 7 and 2 Hz, 3H, SCH(CH$_2$C*H*$_3$)), 1.81−1.97 (m, 2H, SCH(C*H*$_2$CH$_3$)), 1.95 (s, 12H, 4 CH_3CN), 2.47 (s, 3H, CH_3CN trans to S), 2.49 (s, 3H, CH_3CN trans to S), 3.81−3.90 (m, 36H, P(OCH_3)$_3$), 4.75 (m, 1H, SC*H*(CH$_2$CH$_3$)), 6.31 (dd, J = 6 and 1 Hz, 1H, SC*H*=CH)), 6.73 (dd, J = 6 and 4 Hz, 1H, SCH=C*H*)). $^{31}P\{^1H\}$ NMR (CD_3CN, 109 MHz): δ 124.0 and 124.7 (d, $^2J_{PP}$ = 73 Hz), 125.8 (s). $^{13}C\{^1H\}$ NMR (CD_3CN, 68 MHz): δ 4.5 (*C*H$_3$CN trans to S), 12.9 (SCH(CH$_2$*C*H$_3$)), 28.9 (SCH(*C*H$_2$CH$_3$)), 55.6−56.2 (P(O*C*H$_3$)$_3$), 74.4 (S*C*H(CH$_2$CH$_3$)), 126.1 (SCH=*C*H), 135.5 (S*C*H=CH).

Synthesis of [{Ru(P(OCH$_3$)$_3$)$_2$(CH$_3$CN)$_3$}$_2$(μ-SCR^1=CHCHR^{2}S)](CF$_3$SO$_3$)$_4$ (4, R^1 = CH$_3$, R^2 = H; 5, R^1 = CH$_2$CH$_3$, R^2 = CH$_3$; 6, R^1 = C$_6$H$_5$, R^2 = H). Complexes **4**−**6** were synthesized by the procedure analogous to **2**. Thus only the spectroscopic and elemental analysis data are given below.

4: yield 64.0 mg, 0.038 mmol, 48% (from **1** (126.1 mg, 0.079 mmol)). Anal. Calcd for $C_{32}H_{60}F_{12}N_6O_{24}P_4Ru_2S_6$: C, 23.16; H, 3.64; N, 5.06. Found: C, 23.19; H, 3.48; N, 4.94. ^1H NMR (270 MHz, CD_3CN): δ 1.95 (s, 12H, 4 CH_3CN), 2.08 (s, 3H, CH_3C=CH), 2.49 (s, 3H, CH_3CN), 2.50 (s, 3H, CH_3CN), 3.8−4.0 (m, 36H, P(OCH_3)$_3$), 4.08 (ddd, J = 14, 3, and 0.5 Hz, 1H, CHC*H*′S), 4.52 (dt, J = 14 and 2 Hz, 1H, CHCH*H*′S), 6.55 (m, 1H, SC=C*H*CH$_2$). $^{31}P\{^1H\}$ NMR (109 MHz, CD_3CN): δ 124.9 and 125.9 (d, $^2J_{PP}$ = 77 Hz), 125.4 and 125.9 (d, $^2J_{PP}$ = 76 Hz). $^{13}C\{^1H\}$ NMR (CD_3CN, 68 MHz) δ 4.5 (*C*H$_3$CN trans to S), 16.3 (SC(*C*H$_3$)=CH), 52.0 (S*C*H$_2$), 55.3−56.0 (P(O*C*H$_3$)$_3$), 131.3 (SC(CH$_3$)=*C*H), 138.1 (S*C*(CH$_3$)=CH).

5: yield 62.2 mg, 0.037 mmol, 74% (from **1** (80.3 mg, 0.050 mmol)). Anal. Calcd for $C_{34}H_{64}F_{12}N_6O_{24}P_4Ru_2S_6$: C, 24.20; H, 3.82; N, 4.98. Found: C, 24.08; H, 3.65; N, 4.78. ^1H NMR (270 MHz, CD_3CN): δ 1.19 (t, J = 7 Hz, 3H, SCCH$_2$C*H*$_3$), 1.57 (d, J = 7 Hz, 3H, SCHC*H*$_3$), 1.95 (s, 12H, 4 CH_3CN), 2.16 (m, 1 H, CH$_3$C*H*H′CS), 2.50 (s, 3H, CH_3CN), 2.52 (s, 3H, CH_3CN), 2.52 (m, 1H, CH$_3$CH*H*′CS), 3.8−4.0 (m, 36H, P(OCH_3)$_3$), 4.80 (m, 1H, SC*H*CH$_3$), 6.38 (m, 1H, SC=C*H*CH(CH$_3$)S). $^{31}P\{^1H\}$ NMR (109 MHz, CD_3CN): δ 124.1 and 124.8 (d, $^2J_{PP}$ = 75 Hz), 125.6 and 126.3 (d, $^3J_{PP}$ = 78 Hz). $^{13}C\{^1H\}$ NMR (CD_3CN, 68 MHz): δ 4.6 (*C*H$_3$CN trans to S), 14.4 (SC(CH$_2$*C*H$_3$)=CH), 19.7 (SCH(*C*H$_3$)), 24.0 (SC(*C*H$_2$CH$_3$)=CH), 55.6−56.1 (P(O*C*H$_3$)$_3$), 68.1 (S*C*H(CH$_3$)), 132.5 (SC(CH$_2$CH$_3$)=*C*H), 142.4 (S*C*(CH$_2$CH$_3$)=CH).

6: yield 44.2 mg, 0.026 mmol, 52% (from **1** (80.3 mg, 0.050 mmol)). Anal. Calcd for $C_{37}H_{62}F_{12}N_6O_{24}P_4Ru_2S_6$: C, 25.82; H, 3.63; N, 4.88. Found: C, 25.84; H, 3.36; N, 4.55. ^1H NMR (270 MHz, CD_3CN): δ 1.95 (s, 12H, 4 CH_3CN), 2.45 (s, 3H, CH_3CN), 2.47 (s, 3H, CH_3CN), 3.63 (d, $^3J_{PH}$ = 11 Hz, 9H, P(OCH_3)$_3$), 3.8−3.9 (m, 27H, P(OCH_3)$_3$), 4.31 (m, 1H, SC*H*H′), 4.77 (m, 1H, SCH*H*′), 7.12 (m, 1H, SCH$_2$=C*H*), 7.50−7.58 (5H, m, C$_6H_5$). $^{31}P\{^1H\}$ NMR (109 MHz, CD_3CN): δ 123.9 and 125.3 (d, $^2J_{PP}$ = 78 Hz), 125.2 (s).$^{13}C\{^1H\}$ NMR (CD_3CN, 68 MHz): δ 4.5 (*C*H$_3$CN trans to S), 52.2 (S*C*H$_2$), 55.5−55.9 (P(O*C*H$_3$)$_3$), 131.4 (SCH$_2$=*C*H), 131.8 (S*C*(C$_6$H$_5$)), 129.3, 129.7, and 130.5 (*C*$_6$H$_5$).

Reaction of 1 with 2-Pentyne. The reaction was carried out according to the procedures for **2**−**6** at temperatures of 0 and 40 °C. Each batch was recrystallized from CH_3CN/DME. The two products having the same elemental constitution, [{Ru(P(OCH$_3$)$_3$)$_2$(CH$_3$CN)$_3$}$_2${μ-SC(CH$_3$)=CHCH(CH$_3$)S}](CF$_3$SO$_3$)$_4$ (**7**) and [{Ru(P(OCH$_3$)$_3$)$_2$(CH$_3$CN)$_3$}$_2${μ-SC(CH$_2$CH$_3$)=CHCH$_2$S}](CF$_3$SO$_3$)$_4$ (**8**), were obtained as a mixture and were identified with ^1H NMR spectroscopy. The relative abundances of **7** and **8** were determined with ^1H NMR spectroscopy. The yields of the mixture of **7** and **8** at respective temperature were as follows: 25% (22.5 mg, 0.013 mmol) based on **1** (85.2 mg, 0.053 mmol) at 0 °C and 14% (12.1 mg, 0.0072 mmol) based on **1** (80.3 mg, 0.050 mmol) at 40 °C. The elemental analysis of the mixture was also carried out. Anal. Calcd for $C_{33}H_{62}F_{12}N_6O_{24}P_4Ru_2S_6$: C, 23.69; H, 3.73; N, 5.02. Found: C, 23.58; H, 3.58; N, 4.88.

7: ^1H NMR (270 MHz, CD_3CN): δ 1.55 (d, J = 7 Hz, 3H, SC(CH$_3$)=CHCH(C*H*$_3$S)), 1.95 (s, 12H, 4 CH_3CN), 2.05 (s, 3H, SC(C*H*$_3$)=CHCH(CH$_3$)S)), 2.50 (s, 3H, CH_3CN), 2.52 (s, 3H, CH_3CN), 3.84−3.96 (m, 36H, P(OCH_3)$_3$), 4.75 (m, 1H, SC(CH$_3$)=CHC*H*(CH$_3$)S)), 6.39 (m, 1H, SC(CH$_3$)=C*H*CH(CH$_3$)S).

8: ^1H NMR (270 MHz, CD_3CN): δ 1.22 (t, J = 7 Hz, 3H, SCH$_2$CH=C(CH$_2$C*H*$_3$)S), 1.93 (m, 1H, SCH$_2$CH=C(C*H*H′CH$_3$)S, overlapped with CD$_2$*H*CN), 1.95 (s, 12H, 4 CH_3CN), 2.18 (m, 1H, SCH$_2$CH=C(CH*H*′CH$_3$)S), 2.50 (s, 3H, CH_3CN), 2.51 (s, 3H, CH_3CN), 3.83−3.89 (m, 36H, P(OCH_3)$_3$), 4.07 (m, 1H, SC*H*H′CH=C(CH$_2$CH$_3$)S), 4.56 (m, 1H, SCH*H*′CH=C(CH$_2$CH$_3$)S), 6.53 (m, 1H, SCH$_2$C*H*=C(CH$_2$CH$_3$)S).

Table 1. Summary of Crystallographic Data

	2	**3**	**4**	**5**·($C_4H_{10}O_2$)
formula	$C_{37}H_{62}F_{12}N_6O_{24}P_4Ru_2S_7$	$C_{33}H_{62}F_{12}N_6O_{24}P_4Ru_2S_6$	$C_{32}H_{60}F_{12}N_6O_{24}P_4Ru_2S_6$	$C_{38}H_{74}F_{12}N_6O_{26}P_4Ru_2S_6$
fw	1753.37	1673.27	1659.24	1777.41
cryst syst	monoclinic	triclinic	triclinic	triclinic
space group	$P2_1/n$ (# 14)	$P\bar{1}$ (# 2)	$P\bar{1}$ (# 2)	$P\bar{1}$ (# 2)
a (Å)	15.049(2)	12.5250(10)	12.6118(7)	12.300(2)
b (Å)	21.692(3)	13.1414(10)	13.5521(8)	13.352(2)
c (Å)	21.847(3)	20.1640(15)	19.9459(11)	23.217(4)
α (deg)		103.9240(10)	104.7260(10)	93.303(3)
β (deg)	88.001(3)	92.159(2)	92.3080(10)	95.792(4)
γ (deg)		91.140(2)	92.3040(10)	110.864(4)
V (Å^3)	7127.3(16)	3217.7(4)	3289.9(3)	3526.7(11)
Z	4	2	2	2
d_{calcd} (g·cm^{-3})	1.634	1.727	1.675	1.674
μ (mm^{-1})	0.821	0.873	0.853	0.804
abs corr	SADABS	SADABS	SADABS	SADABS
no. of reflns (total)	16 281	13 609	14 656	15 573
no. of reflns ($F_o^2 > 2\sigma(F_o^2)$)	6102	9909	6778	6222
no of params	690	674	635	704
R1[a]	0.0856	0.0835	0.0985	0.1177
wR2[b]	0.2199	0.2303	0.2698	0.2913
GOF[c]	0.906	1.047	1.002	0.952

	6	**7**	**8**
formula	$C_{37}H_{62}F_{12}N_6O_{24}P_4Ru_2S_6$	$C_{33}H_{62}F_{12}N_6O_{24}P_4Ru_2S_6$	$C_{33}H_{62}F_{12}N_6O_{24}P_4Ru_2S_6$
fw	1721.31	1673.27	673.27
cryst syst	triclinic	triclinic	triclinic
space group	$P\bar{1}$ (# 2)	$P\bar{1}$ (# 2)	$P\bar{1}$ (# 2)
a (Å)	12.7771(8)	12.6346(10)	12.6158(11)
b (Å)	13.1696(8)	13.5211(11)	13.5141(12)
c (Å)	20.4717(12)	20.8218(17)	20.0622(17)
α (deg)	104.7250(10)	84.677(2)	103.719(2)
β (deg)	90.0780(10)	85.363(2)	91.919(2)
γ (deg)	90.2030(10)	71.596(2)	92.209(2)
V (Å^3)	3331.6(4)	3355.6(5)	3317.2(5)
Z	2	2	2
d_{calcd} (g·cm^{-3})	1.716	1.656	1.675
μ (mm^{-1})	0.846	0.837	0.847
abs corr	SADABS	SADABS	SADABS
no. of reflns (total)	14 884	14 894	14 851
no. of reflns ($F_o^2 > 2\sigma(F_o^2)$)	7747	3654	3758
no of params	678	671	643
R1[a]	0.0743	0.1318	0.1096
wR2[b]	0.1934	0.3422	0.2669
GOF[c]	0.779	0.844	0.806

[a] R1 = $\sum|F_o - F_c|/\sum|F_o|$ for reflections $F_o^2 > 2\sigma(F_o^2)$. [b] wR2 = $[\sum w(F_o^2 - F_c^2)^2/\sum w(F_o^2)^2]^{1/2}$. [c] GOF = $[\sum w(F_o^2 - F_c^2)^2/\sum(n - p)]^{1/2}$.

X-ray Diffraction Studies. The diffraction data for **2**−**8** were collected on a Bruker CCD SMART 1000 diffractometer using Mo Kα radiation. All intensity data were processed by using the SAINT-plus program package. All structure solutions were performed with the SHELXTL software package. Details of the six crystallographic analyses are summarized in Table 1.

Results and Discussion

In the previous study on the reaction of **1** with alkenes, only terminal alkenes reacted with **1** and internal alkenes such as 2-pentene were inert toward **1**. Therefore, **1** was treated with terminal alkynes, such as 1-pentyne and phenylpropargyl sulfide in CH_3CN, to give orange- to red-colored solutions. The standard workup of the solutions gave yellow crystals of [{Ru(P(OCH$_3$)$_3$)$_2$(CH$_3$CN)$_3$}$_2$(μ-SCH=CHCH(R)S}](CF$_3$SO$_3$)$_4$ (**2**, R = SC_6H_5, 63%; **3**, R = C_2H_5, 58%) (eq 1).

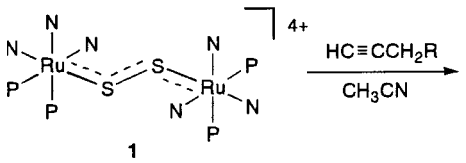

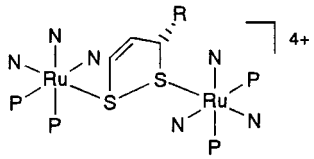

(1)

2: R = SC_6H_5, yellow, 63%
3: R = C_2H_5, yellow, 58%

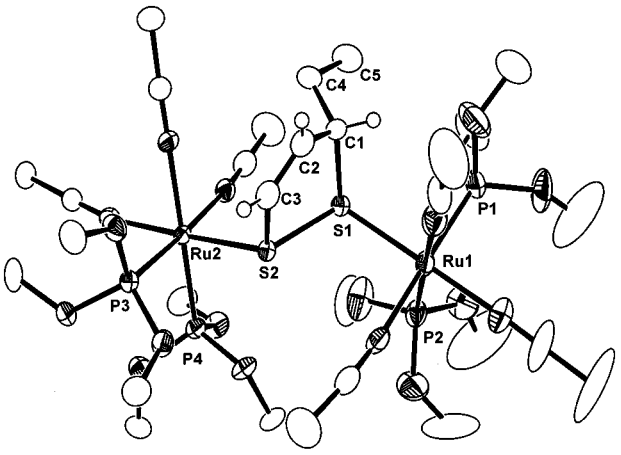

Figure 1. Structure of complex **3** (the cation part, the methyl and aromatic H atoms are omitted for clarity).

Through the reactions, the propargylic C−H bond is cleaved and the H atom is transferred to the neighboring sp^2-hybridized carbon atom, and two C−S bonds are formed. As a result, the dithiacyclopentene framework is formed and bridges the two Ru centers. In the ^{1}H NMR spectrum of **2**, the characteristic signals due to the two olefinic protons and a methyne proton in the dithiacyclopentene ring are observed at δ 6.92 (dd with $^3J_{H1H2}$ = 5.9 Hz and $^3J_{H2H3}$ = 4.0 Hz), 6.47 (dd with $^3J_{H1H2}$ and $^4J_{H1H3}$ = 0.8 Hz), and 6.12 (dd with $^3J_{H2H3}$ and $^4J_{H1H3}$), respectively. Figure 1 shows the structure of **3**, whereas that of **2** is deposited in the Supporting Information.

The two C−C distances in the C_3S_2 framework of C1−C2 (1.466(12) Å) and C2−C3 (1.286(12) Å) are assigned to a single and a double bond, respectively. The S2−C3−C2−C1 torsion angle of 3.7(11)° indicates that the four atoms sit almost on a plane, and the C2 and C3 are sp^2-hybridized carbon atoms. The S1−S2 bond distance of 2.139(3) Å is comparable to those found in the previously reported [{Ru(P(OCH$_3$)$_3$)$_2$(CH$_3$CN)$_3$}$_2$(μ-SCH$_2$CH$_2$CHRS)](CF$_3$SO$_3$)$_4$ (R = C_2H_5, OC_6H_5, and CH=CHCH$_3$, S1−S2: 2.1102(15)−2.164(5) Å),[15] which were synthesized from the reaction of **1** with 1-alkenes and are longer than that of **1** (1.933(11) Å),[16] those in ketonated complexes having one C−S bond (2.040(7)−2.069(4) Å)[17] and typical S−S single and double bonds

Table 2. Selected Bond Distances (Å) and Angles (deg) for 2, 3, 4, 5, and 6

	2	3	4	5	6
		Bond Distances			
Ru1−S1	2.329(2)	2.3528(18)	2.325(3)	2.334(3)	2.3209(19)
Ru2−S2	2.333(2)	2.3244(17)	2.360(3)	2.349(3)	2.3592(19)
Ru1−P1	2.253(3)	2.243(2)	2.252(3)	2.255(4)	2.255(2)
Ru1−P2	2.258(3)	2.252(2)	2.260(3)	2.259(3)	2.253(2)
Ru2−P3	2.267(3)	2.2548(18)	2.252(4)	2.250(3)	2.248(2)
Ru2−P4	2.266(2)	2.2481(18)	2.250(4)	2.246(3)	2.259(2)
S1−S2	2.149(3)	2.139(2)	2.121(4)	2.137(4)	2.119(3)
S1−C1	1.854(9)	1.865(7)	1.809(13)	1.886(12)	1.836(9)
S2−C3	1.751(9)	1.776(8)	1.822(13)	1.791(11)	1.800(9)
C1−C2	1.485(12)	1.466(12)	1.465(19)	1.470(17)	1.473(12)
C2−C3	1.304(12)	1.286(12)	1.257(19)	1.262(16)	1.333(12)
		Bond Angles			
Ru1−S1−S2	106.51(11)	108.35(9)	110.96(14)	108.81(14)	108.96(10)
Ru2−S2−S1	113.01(11)	113.61(9)	108.70(14)	111.42(13)	108.99(10)
Ru1−S1−C1	109.6(3)	110.0(3)	109.5(4)	108.7(4)	109.7(3)
Ru2−S2−C3	110.0(3)	108.7(3)	110.9(4)	110.0(4)	112.9(3)
S1−C1−C2	107.9(6)	107.5(6)	108.1(10)	106.1(8)	107.0(6)
S2−C3−C2	119.2(7)	118.6(7)	115.1(10)	118.4(9)	115.2(6)
		Torsion Angles[a]			
Ru1−S1−S2−Ru2	147.28(9)	152.77(7)	158.03(12)	151.43(11)	159.09(8)
Ru1−S1−C1−C2	93.7(6)	90.0(5)	86.7(8)	93.4(8)	80.8(6)
Ru2−S2−C3−C2	108.0(8)	104.8(7)	93.5(11)	102.5(9)	92.6(6)
S2−C3−C2−C1	3.2(13)	3.7(11)	0.0(18)	1.6(17)	0.9(10)

[a] Reported without the sign.

in the disulfides (2.05 and 1.89 Å).[18] The Ru−S distances (2.3528(18) and 2.3244(17) Å) are longer than those of **1** (2.279(9) and 2.245(9) Å).[16]

In contrast to the inertness of internal alkenes, internal alkynes such as 2-butyne, 3-hexyne, and 1-phenyl-2-propyne react with **1** to give a series of disubstituted dithiacyclopentene complexes, $[\{Ru(P(OCH_3)_3)_2(CH_3CN)_3\}_2(\mu\text{-}SCR^1{=}CHCHR^2S)](CF_3SO_3)_4$ (**4**, $R^1 = CH_3$, $R^2 = H$, 48%; **5**, $R^1 = CH_2CH_3$, $R^2 = CH_3$, 70%; **6**, $R^1 = C_6H_5$, $R^2 = H$, 52%) (eq 2).

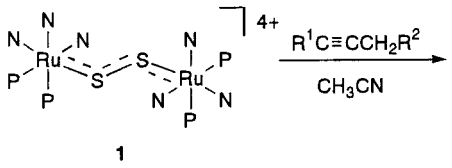

1

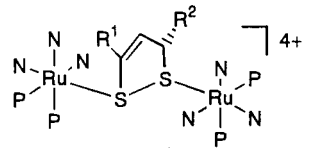

(2)

4: $R^1 = CH_3$, $R^2 = H$, 48 %

5: $R^1 = CH_2CH_3$, $R^2 = CH_3$, 70 %

6: $R^1 = C_6H_5$, $R^2 = H$, 52 %

Complexes **4**−**6** were successfully isolated as crystalline materials and were fully characterized by X-ray analysis. The selected structural parameters are summarized in Table 2 together with those of **2** and **3**. Complexes **4**, **5**, and **6** were more easily purified than **2** and **3**: after the reaction, the remaining excess terminal alkyne seems to decompose the product in the reaction mixture, whereas the internal alkyne is inert toward the product, and therefore the purification is easier. The X-ray structural analysis of **4**, **5**, and **6** confirmed the formation of a dithiacyclopentene ring. The structure of **4** is shown in Figure 2.

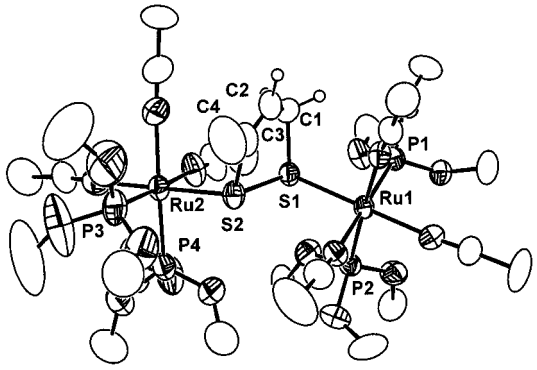

Figure 2. Structure of complex **4** (the cation part, the methyl H atoms are omitted for clarity).

The long C1−C2 and short C2−C3 distances are assigned to single and double C−C bond distances. Since the S2−C3−C2−C1 torsion angle is close to 0°, the C3 and C2 are sp^2-hybridized carbon atoms in each case. Since the propargylic C−H bonds in 2-butyne and 3-hexyne are chemically equivalent, the single products **4** and **5** were obtained, respectively. Complex **6** was also obtained as a sole product via methyl C−H bond activation. We attempted a similar reaction with $C_6H_5C{\equiv}CCD_3$ to obtain **6**-d_3; however, the isolation was not successful, since the product did not give the expected ^{1}H NMR spectrum. A significant primary kinetic isotope effect is reported at the stage of the C−H bond activation in the reaction of **1**-d_{18} (CD_3CN-substituted **1**) with 1-pentene-3,3-d_2 (estimated $k_H/k_D = 9$).[15] This isotopic effect suggests the mechanism that the C−S bond formation on **1** is initiated by the activation of the appropriate C−H bond of the ketones and alkenes. When the C−H bond is replaced by a C−D bond, the initial step is hampered due to the isotope effect, and

(16) Matsumoto, K.; Matsumoto, T.; Kawano, M.; Ohnuki, H.; Shichi, Y.; Nishide, T.; Sato, T. *J. Am. Chem. Soc.* **1996**, *118*, 3597.

(17) (a) Matsumoto, K.; Uemura, H.; Kawano, M. *Inorg. Chem.* **1995**, *34*, 658. (b) Sugiyama, H.; Hossain, Md., M.; Lin, Y.-S.; Matsumoto, K. *Inorg. Chem.* **2000**, *39*, 3948.

(18) Kuczkowski, R. L. *J. Am. Chem. Soc.* **1964**, *86*, 3617.

Scheme 1

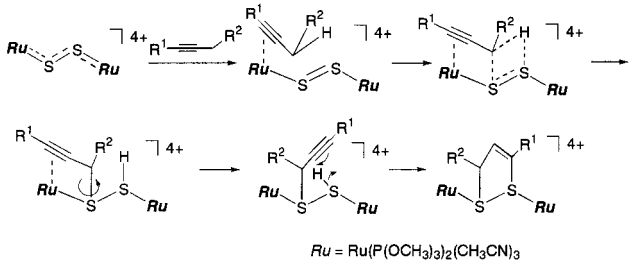

Scheme 2

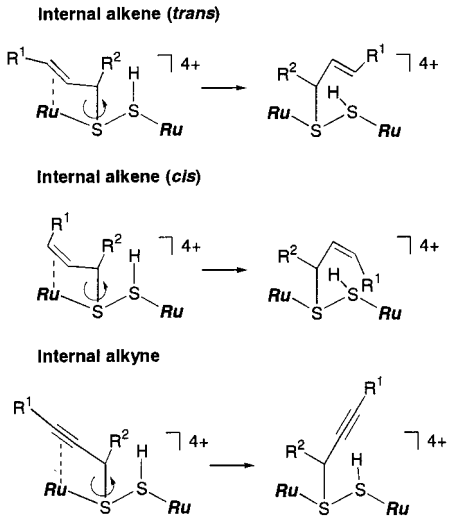

the contribution of the unidentified side reaction may become significant. The mechanism for the cyclization reaction of the alkyne with the S_2 in **1** is shown in Scheme 1. For the internal alkenes, the rotation of the C−S bond in Scheme 1 seems to be hindered by the bulky substituent on the ligands, and therefore the reaction does not proceed. In contrast, the substituent groups in internal alkynes are separated from the coordination sphere due to the linear C≡C triple bond, and the reaction is less hindered (Scheme 2).

When an unsymmetric alkyne having two different propargylic C−H bonds is used, two possible compounds are expected to form. The reaction of **1** with 2-pentyne gave a mixture of complexes [{$Ru(P(OCH_3)_3)_2(CH_3CN)_3$}$_2$ {μ-SC(CH_3)=CHCH(CH_3)S}](CF_3SO_3)$_4$ (**7**) and [{$Ru(P(OCH_3)_3)_2(CH_3CN)_3$}$_2${$\mu$-SC($CH_2CH_3$)=CH-$CH_2$S}]($CF_3SO_3$)$_4$ (**8**), as a result of the C−H bond activation at the methylene and methyl group, respectively (eq 3).

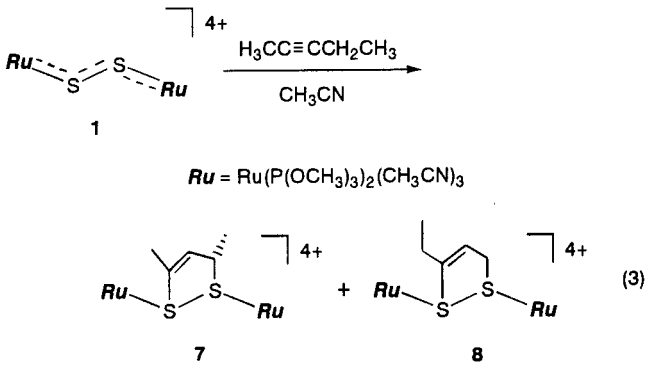

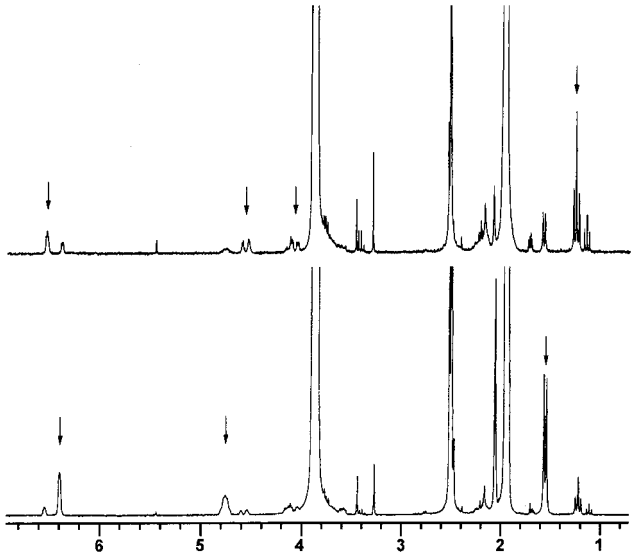

Figure 3. ^{1}H NMR spectra of the once precipitated mixture of **7** and **8** obtained at 40 °C (top) and 0 °C (bottom) in CD_3CN. Arrowed peaks arise from the major products at the respective temperature.

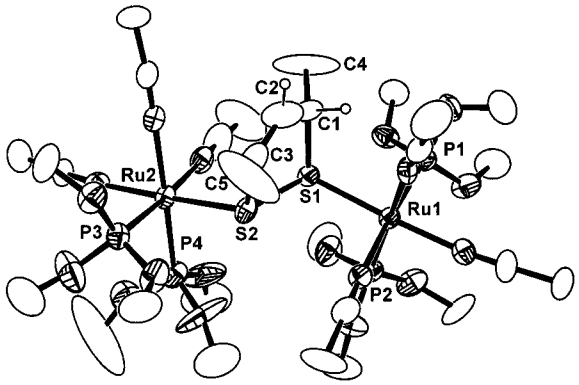

Figure 4. Structure of complex **7** (the cation part, the methyl H atoms are omitted for clarity).

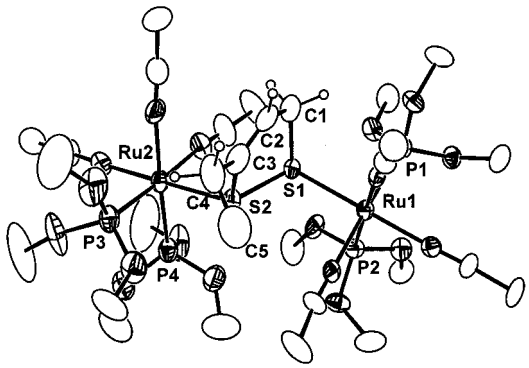

Figure 5. Structure of complex **8** (the cation part, the methyl H atoms are omitted for clarity).

The molar ratio of **7**/**8** was dependent on the reaction temperature. The signals of both **7** and **8** were monitored with ^{1}H and ^{31}P{^{1}H} NMR spectroscopy, and the ^{1}H NMR spectra at 40 and 0 °C are shown in Figure 3.

The olefin proton resonances are observed at δ 6.39 for **7** and δ 6.53 for **8**. Their integrated intensities were used for the determination of the **8**/**7** ratio. Compound **7** is preferably formed at lower temperature, whereas **8** is more abundantly formed at higher temperature, as

Table 3. Selected Structural Parameters for 7 and 8

	7	8
	Bond Distances (Å)	
Ru1−S1	2.342(5)	2.327(4)
Ru2−S2	2.337(5)	2.374(4)
Ru1−P1	2.257(5)	2.244(4)
Ru1−P2	2.256(5)	2.251(4)
Ru2−P3	2.252(5)	2.247(5)
Ru2−P4	2.250(6)	2.249(5)
S1−S2	2.123(6)	2.119(6)
S1−C1	1.84(2)	1.85(2)
S2−C3	1.81(2)	1.85(2)
C1−C2	1.38(3)	1.42(3)
C2−C3	1.32(3)	1.29(3)
	Bond Angles (deg)	
Ru1−S1−S2	111.2(2)	111.6(2)
Ru2−S2−S1	110.7(2)	108.5(2)
Ru1−S1−C1	108.8(7)	109.8(6)
Ru2−S2−C3	109.4(7)	109.5(6)
S1−C1−C2	110.5(17)	108.0(16)
S2−C3−C2	114.4(18)	114.1(16)
	Torsion Angles[a] (deg)	
Ru1−S1−S2−Ru2	154.63(18)	156.42(17)
Ru1−S1−C1−C2	94.9(16)	89.4(13)
Ru2−S2−C3−C2	95.8(17)	95.6(15)
S2−C3−C2−C1	7(3)	2(3)

[a] Reported without the sign.

the **8**/**7** ratios of 0.18 at 0 and 2.4 at 40 °C show. Similar temperature-dependent selectivity was found in the reaction of **1** with butanone as described in the previous report, in which the keto-C−H bond is more favorably cleaved in the order 1° > 2° at 40 °C, whereas the order is reversed at 0 °C.[17] From the present temperature-dependent results, it is conceived that the rotation of the C−S bond in Scheme 1 also affects the product distribution as well as the C−H bond activation. On this assumption, it is reasonable that the approach of the C−H bond to the S_2 in Scheme 1 is less favorable for the bulkier ethylpropargyl group at high temperatures and **8** becomes the dominant product.

It was difficult to obtain selectively either **7** or **8** only by varying the temperature. However, both crystals of **7** and **8** suitable for X-ray analysis were picked up from the **7**-rich and the **8**-rich samples to obtain their structures as shown in Figures 4 and 5, respectively. The selected structural parameters are listed in Table 2, and these are comparable to those of **2**−**6**.

Conclusion

Complex **1** reacts with both terminal and internal alkynes to give a series of C_3S_2 ring complexes via activation of the propargylic C−H bond. The reaction mechanism is basically parallel to the alkene reactions except that both internal and terminal alkynes react, whereas only terminal alkenes react with **1**.

Acknowledgment. The financial support of CREST from Japan Science and Technology Corporation and the Grant-in-Aid for COE Research, Ministry of Education, Culture, Sports, Science and Technology (MEXT), are acknowledged.

Supporting Information Available: X-ray crystallographic files for the determinations of **2**−**8**, and tables and figures with full numbering schemes. This material is available free of charge via the Internet at http://pubs.acs.org.

OM0106534